LWS grating resolution and line profiles

Cecile Gry, Rosario Lorente

November 15, 2000

1 Introduction

This document presents the line profile properties for the grating mode of the ISO Long Wavelength Spectrometer (LWS). This work has been performed in the frame of the Line Profile Working Group, created in September 1998.

2 Calibration sources and types of observations

To characterize the line profiles, we have used the same observations as for the wavelength calibration. The wavelength standards had been chosen so as to provide the largest possible sample of strong and narrow lines and so that several of them are visible from ISO as much as possible during the mission. The chosen sources are mainly planetary nebulae and HII regions. Table 1 lists the sources available for each of the atomic lines used to characterize the profiles. Figure 1 shows the time coverage of the calibration sources throughout the mission.

The observations are performed weekly with end-to-end grating scans and provide measurements of seven different emission lines, spread between 51 μm and 158 μm, and appearing on two detectors each.

Note that there are no measurements for SW4 and LW5, as no strong line was found in their wavelength range.

The observation have been performed in a homogeneous way from revolution 342 onwards, with AOT L01, with 3 forward and 3 backward scans, and an oversampling of 8. Before revolution 342, many AOT observations were not performed with an equal number of forward and backward scans, and during PV phase the observations were performed with COIFs, generally with a higher number of scans and a higher oversampling. Some of them were short scans over a limited number of lines. In order to have an homogeneous sampling, only those data obtained with AOT L01, an oversampling of 8, 6 scans of the full grating range and the same number of forward and backward scans were used.

3 Preparation of the data

The data processing has been performed with the ISAP software. The following scheme summarizes the standard processing of the selected observations :

Table 1: *Lines from astronomical sources performed for grating wavelength calibration and line profile characterisation.*

line $\lambda\,[\mu m]$	**det**	**LVDT** mean(σ)	**# obs**	**sources**
[OIII]51.815	SW1	1327(3)	171	NGC6543 NGC6826 G298.228 IRAS15408 NGC7027
[OIII]51.815	SW2	2783(3)	196	NGC6543 NGC6826 G298.228 IRAS15408 NGC7027 NGC6302
[NIII]57.330	SW2	1993(2)	161	NGC6543 NGC6826 G298.228 IRAS15408 NGC6302
[NIII]57.330	SW3	3376(5)	152	G298.228 IRAS15408 NGC6302
[OI]63.184	SW2	1124(3)	88	G298.228 IRAS15408 NGC7027 NGC6302 NGC7023 IRAS23133
[OI]63.184	SW3	2584(3)	97	G298.228 IRAS15408 NGC7027 NGC6302 NGC7023 IRAS23133
[OIII]88.356	SW5	1579(3)	185	NGC6543 NGC6826 G298.228 IRAS15408 NGC7027 NGC6302
[OIII]88.356	LW1	3142(4)	189	NGC6543 NGC6826 G298.228 IRAS15408 NGC7027, NGC6302
[NII]121.889	LW2	2176(2)	7	NGC6302
[OI]145.525	LW3	1878(4)	76	G298.228 IRAS15408 NGC7027 NGC7023 IRAS23133
[OI]145.525	LW4	3250(5)	80	G298.228 IRAS15408 NGC7027 NGC6302 NGC7023 IRAS23133
[CII]157.741	LW3	945(4)	90	G298.228 IRAS15408 NGC7027 NGC6302 NGC7023 IRAS23133
[CII]157.741	LW4	2374(3)	91	G298.228 IRAS15408 NGC7027 NGC6302 NGC7023 IRAS23133

- For each object we selected up to 20 observations well spread all over the mission.
- Each individual scan was checked for the presence of glitches or any anomalous feature. Glitches have been removed and anomalous scans have been discarded.
- Each scan has been rebinned to 32 points per resolution element.
- Forward and backward scans have been averaged separately.
- For extended sources, the resulting scans have been corrected for the presence of fringes.
- The continuum has been fitted by a polynomial and subtracted off.

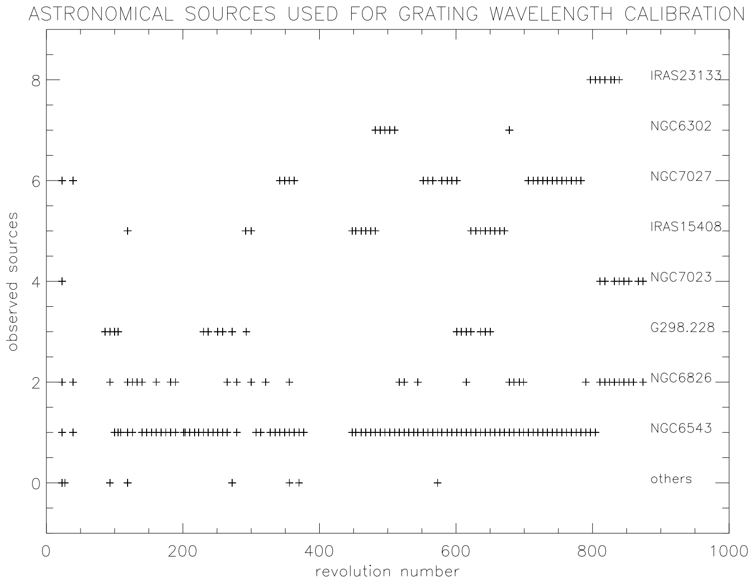

Figure 1: *Main LWS grating wavelength standards observed during the mission. The gap between revolutions 378 and 442 corresponds to the period when LWS was not used because of a problem with the FP interchange wheel.*

- The profiles have been normalized to a peak value of one.
- The resulting spectra have been re-centered on the laboratory wavelength, so that profiles from different velocity sources can be compared.

The products were thus one spectrum per scan direction per spectral line per detector per observation per object.

4 Stability of the line profiles

In order to define as general a profile as possible, we looked for the effects of each parameter susceptible of inducing profile variations in a step by step approach. When a parameter had proved not to induce any significant variation, the profiles were averaged over this parameter for the subsequent study.

4.1 Stability with time

All observations of the same line on the same detector for the same object have been plotted together to look for time variations. The peak to peak variations in the peak height of the line were as low as 2% for the bright lines and always less than 20% in the worst cases corresponding to the faintest lines used. The variation of the line width with time is much smaller than the sampling interval of the observations (8 points per resolution element), except for a few cases of a faint line with a low line/continuum ratio, where the width is more difficult to assess.

In any case, for both the peak height and the width, no trend was found with time and we conclude that the observed dispersion shows the limits of the photometric accuracy of the LWS detectors and there are no significant time variation in the instrumental profiles.

For subsequent steps, the data were thus averaged on time, i. e. all observations of the same line in the same object, recorded with the same scan direction on the same detector, were averaged together.

4.2 Search for transient effects : comparison of forward and backward scans

Any transient or memory effect affecting the grating profiles would create differences between the profiles recorded in the two opposite directions, forward and backward. In the absence of any availble transient correction procedure (which hopefully will be available in the course of the year 2001), we have to check if the scan direction is inducing a significant variation in the line profiles. Indeed at the peak and feet of the lines, some differences appear between forward and backward scans for the same line from the same object. The difference in the peak is always less than 2% in the case of the short wavelength detectors, and can be up to 6% for the long wavelength detectors. In most cases the backward scan is higher than the forward one, but the contrary also occurs, especially (but not automatically) when the continuum is steeper. There is no trend with flux level. Therefore these differences seem to be due to more than one effect. In the line feet, at the continuum level, a line broadening can be observed, in general to the left for forward scans and to the right for backward scans. The opposite is also seen though, possibly due to uncertainties in placing the continuum. In general the transients have a symetrical effect in forward and backward scans, so that the line is broadened symetrically if the observations have been performed in both directions and all scans are added together.

Because of this symetry, and because most of the difference between forward and backward scans are seen in the feet of the line, where they can easily be confused with continuum features and thereby where they can easily be removed by the baseline subtraction process, our recommendation is, as long as no formal transient correction is available, to use both scan directions together. We have thus averaged forward and backward profiles for the rest of the study.

4.3 Variation of line profile with object (and thereby line strength)

In figures 2 and 3 the profiles are shown for each line/detector combination, all objects presenting the line being overplotted on each other. We still have two separate samples for point and extended sources.

In general the profiles show very little difference from object to object (the differences are less than 4%). Only in three cases some differences appear :

- the $145\mu m$ line on detector LW3. It is a faint line in the objects we are dealing with, therefore the differences could be due to noise and problem

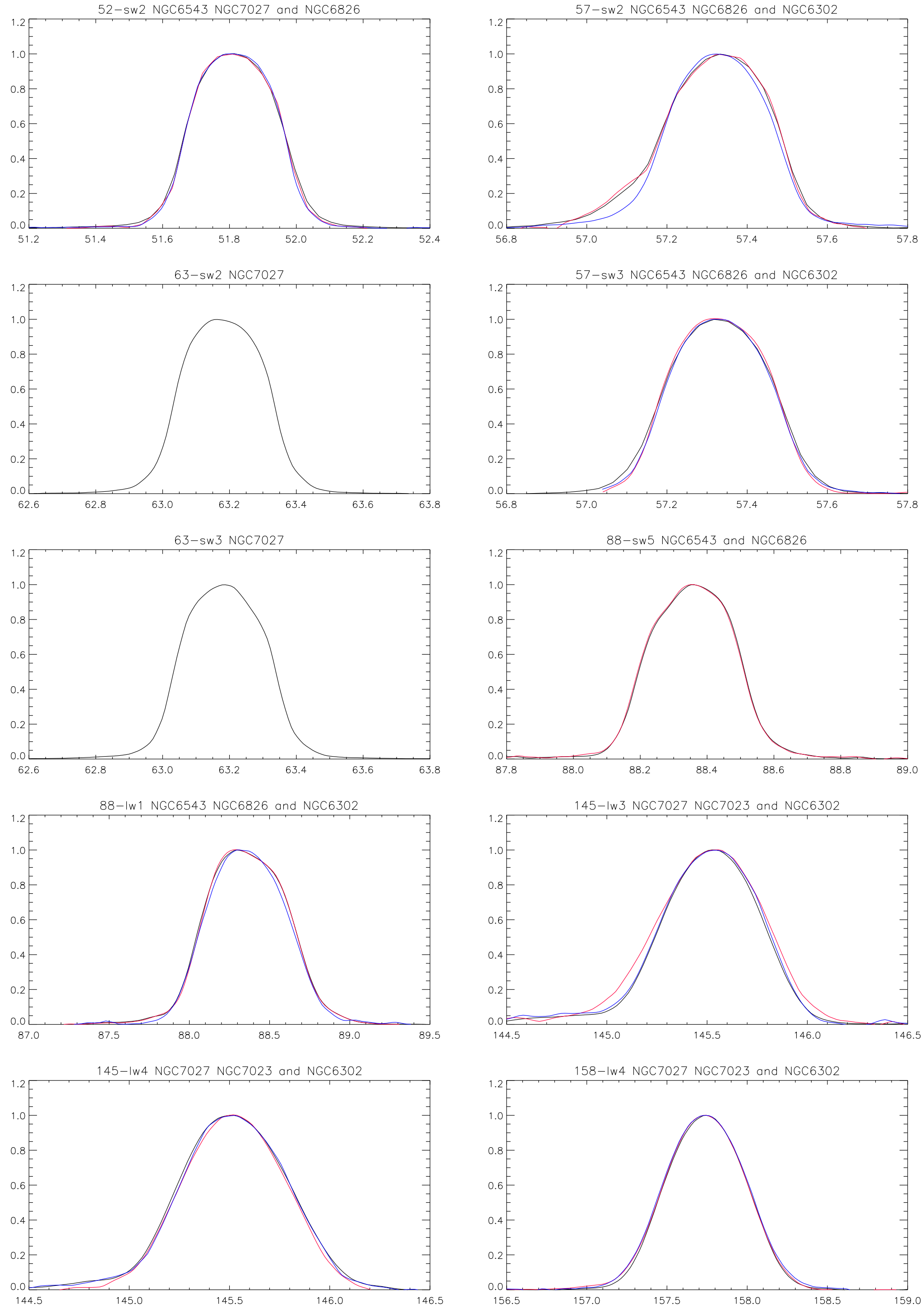

Figure 2: *Lines studied for point sources. On top of each pannel the list of objects is indicated. The color code is as follows: black : first object in the list, red : second object, blue : third object.*

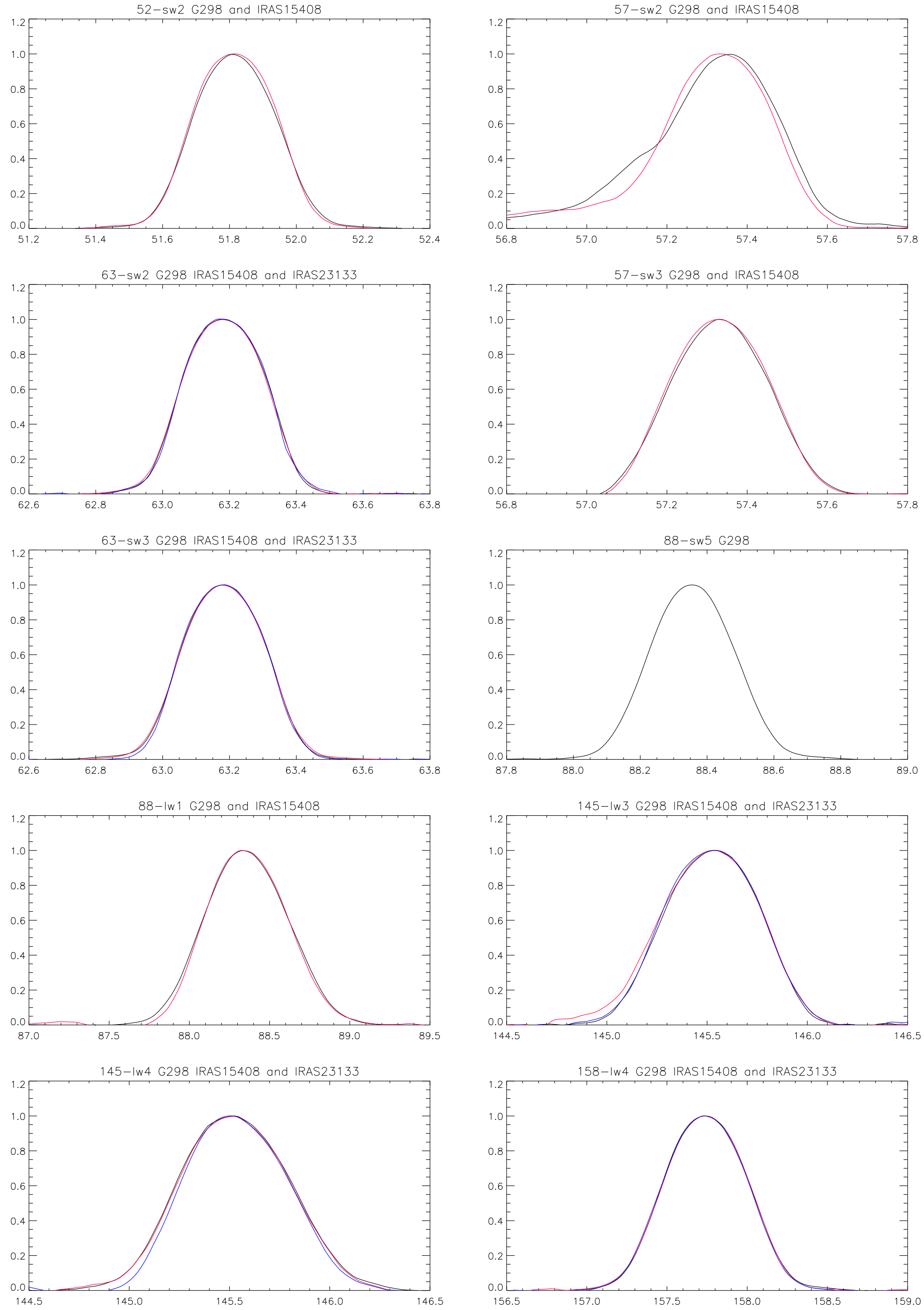

Figure 3: *Lines studied for extended sources. Same color code as in previous figure.*

in the baseline subtraction.

- the $88 \mu m$ line on detector LW1. In this case two objects (NGC6543 and NGC6302) show identical but assymmetrical profiles, while NGC6826 shows a more symmetrical profile. We have not found any reason for this behavior (no relation with the object type or line saturation etc...). But in any case the differences are smaller than the dispersion with time mentionned at the begining of our study and are nor significant.

- the $57 \mu m$ line on detector SW2. It is clearly an anomalous line, very assymmetrical on the blue edge. The difference between the different objects occurs in this assymmetry. As we will see in the next section, this line is clearly anomalous on SW2 and will be kept out of the general profile determination.

In consequence, it appears that the profile is stable among the considered objects and we average the profiles over the different objects, creating a unique profile per spectral line and detector.

4.4 Comparison of profiles on different detectors

Figure 4 shows the profiles for all detectors plotted on top of each other, for both point and extended sources.

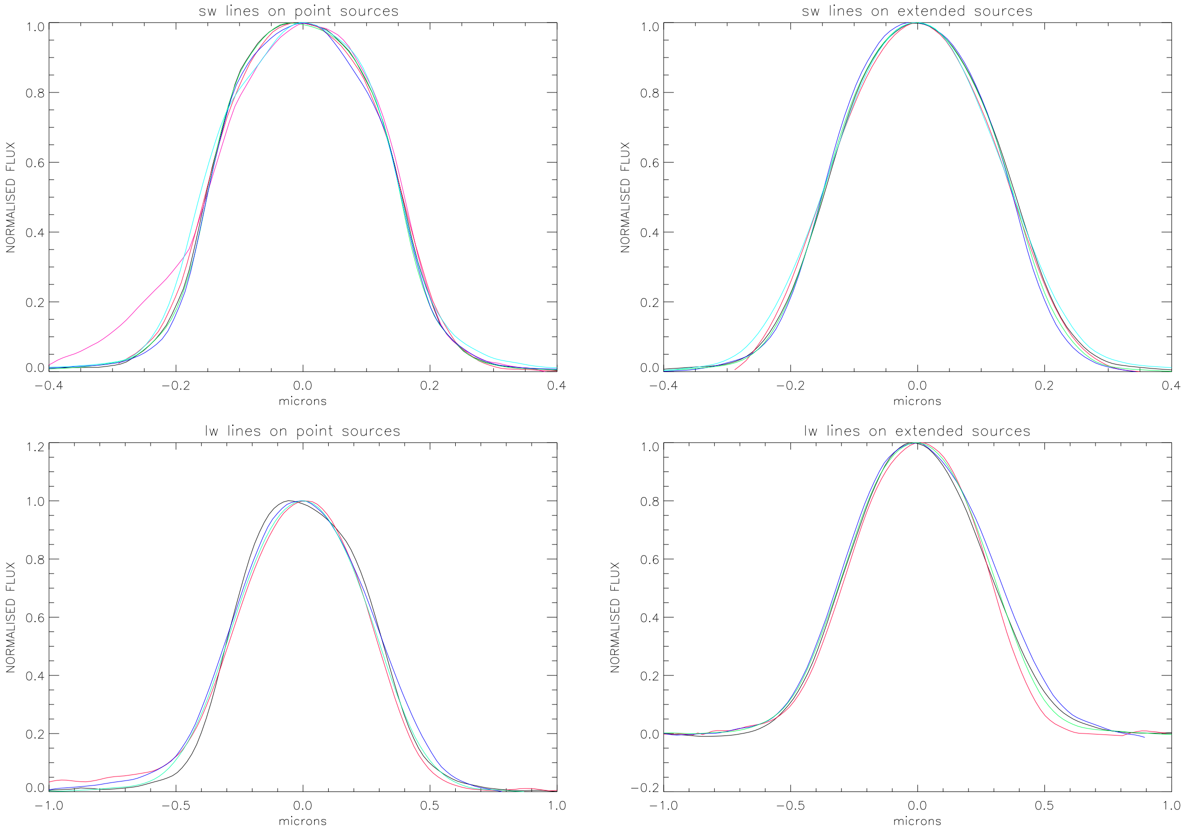

Figure 4: *Comparison of profiles on different detectors. The profiles have been averaged over different objects, resulting in one profile (i.e. one colour in the plot) per line per detector.*

They show no significant differences between lines coming from different detectors except for the anomalous case of the $57\mu m$ line on detector SW2, which shows a strong asymmetry toward the short wavelengths. The asymmetry is clearly not real because it does not appear when the same line is observed with the detector SW3. It is not due to the detector either, as two other lines falling on SW2 (at $52\mu m$ and $63\mu m$) do not show any anomaly. However the presence and the strength of the asymmetry is object-dependent. It seems to be related to the presence of a "ghost" line shortward of the NIII $57\mu m$ line on detector SW2 in the Fabry-Perot spectrum (see LWS Handbook Section 5.8). The $57\mu m$ line on detector SW2 is excluded from the mean profile obtained by averaging all lines from all detectors.

4.5 Difference in line profiles from point and extended sources

The reason for keeping the profiles from extended sources separate from the point source profiles was for checking that the problems related to off-centered emission did not create any distortion in the line profiles. Figure 5 shows that, if anything, the profiles from the extended sources are more symmetrical and more similar to a gaussian than the point source profiles. We thus conclude that there is no distortion coming from the source extension or off-centering.

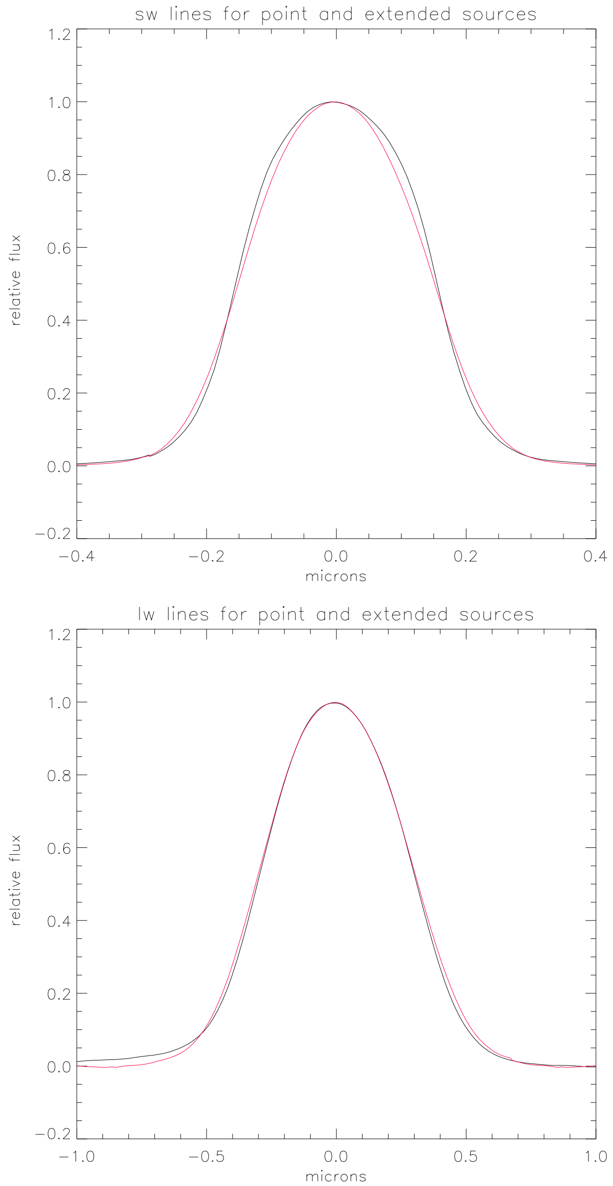

Figure 5: *Mean profiles for point (black) and extended (red) sources.*

5 Comparison with a gaussian profile

When taking into account all the LWS optical elements and the detector characteristics, the wavelength response function is not expected to be gaussian. it is however always convenient when measuring a line intensity to be able to use a gaussian aproximation. Figure 6 shows the comparison of the measured mean profiles with gaussian functions fitted to them. They also show the residuals, i.e. the differences between the two profiles.
Table 2 lists the line flux, full width at half maximum and peak heights for the measured profiles and for the fitted gaussian. This shows that the error made on the determination of the flux with a gaussian fit is of the order of 2%.
The line full widths at half maximum that we measure on our profiles are slightly larger than those measured before launch : 0.31 instead of 0.29 for the short wavelength detectors, and 0.61 instead of 0.60 for the long wavelength detectors. This could be due to the broadening effect of transients.

Table 2: *Parameters of the computed grating profiles compared with the results of the Gaussian fits to the profiles.*

det.	FWHM	line flux	height	FWHM (Gaussian)	line flux (Gaussian)	height (Gaussian)
SW	$.308 \pm .005$	$.314 \pm .008$	1.00	$.283 \pm .009$	$.322 \pm .01$	$1.06 \pm .02$
LW	$.611 \pm .014$	$.637 \pm .014$	1.00	$.584 \pm .015$	$.644 \pm .016$	$1.04 \pm .02$

6 Effect of a lower spectral sampling

The above study of the line profile has been conducted with the highest oversampling permitted in the observations, an oversamping of 8, i.e. 8 points per spectral element, to define as well as possible the true profiles of the instrument. However, in AOT L01 and L02 four different oversampling were permitted : 8, 4, 2 and 1. Following the Nyquist theorem, an oversampling of 2 or higher allows to derive the line flux with a precision better than 5%. (A sampling of 1 point per spectral resolution element is clearly insufficient.) However, we would like to warn the user that a Gaussian fit performed to observations obtained with an oversampling of 2 or even 4 might give results with a higher error than the one quoted above for an oversampling of 8. This is due to the fact that when a line is scanned quickly, the transient effects can be more important and would tend to broaden the line. This effect should be reduced once a transient correction is available.

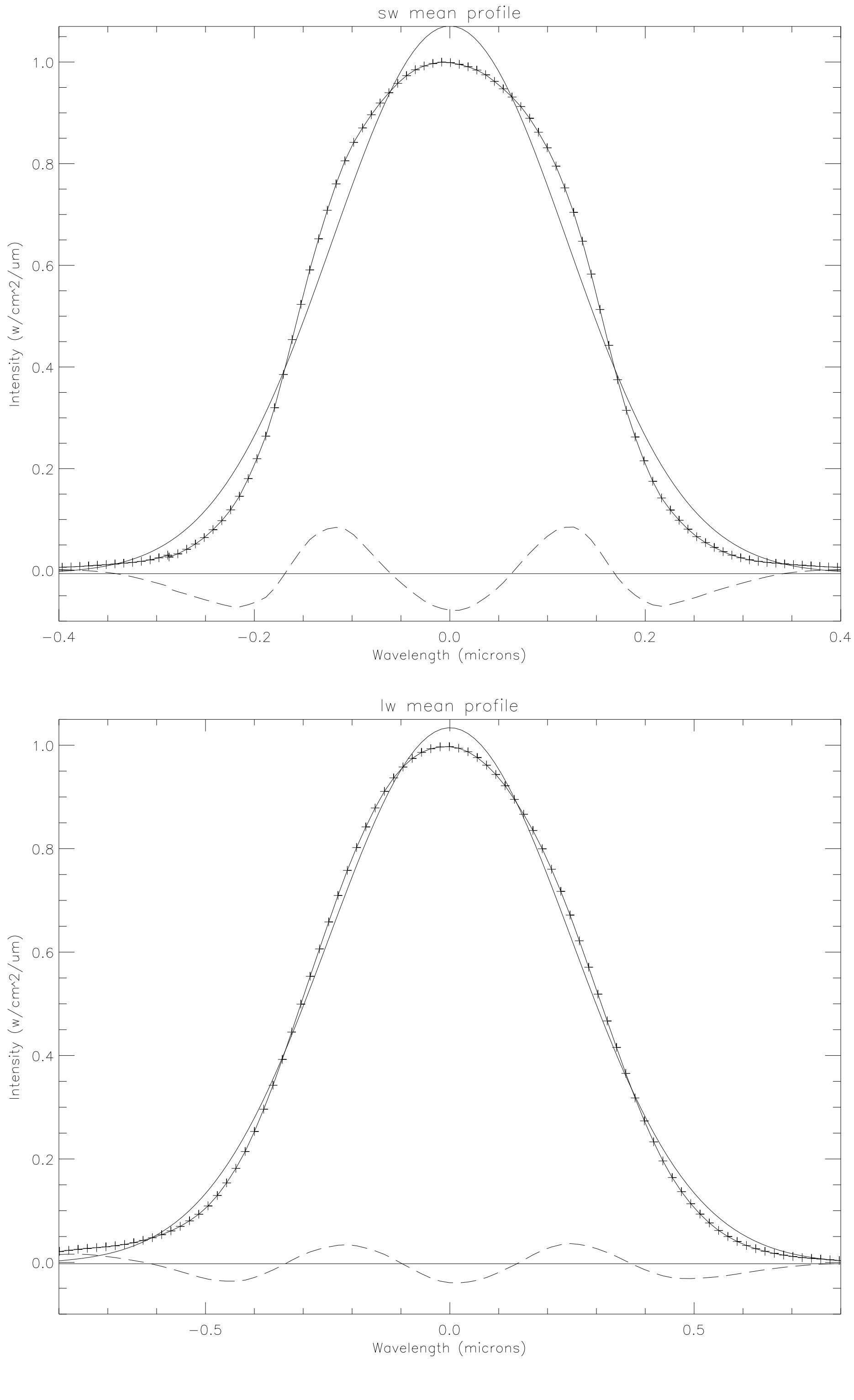

Figure 6: *Measured grating profile (crosses) for short wavelength detectors SW1 to SW5 (top) and long wavelength detectors LW1 to LW5 (bottom) and comparison with gaussian fits (solid line). The residuals i.e. the differences between the measured profile and the gaussian fit are also shown (dashed line).*